ISSN: 2279 - 0594

Journal of Biomedical and Pharmaceutical Research

Available Online at www.jbpr.in

CODEN: - JBPRAU (Source: - American Chemical Society)

Index Copernicus Value: 63.24

PubMed (National Library of Medicine): ID: (101671502)

Volume 6, Issue 1: January-February: 2017, 09-17

Research Article

ELECTROCHEMICAL PEROXIDASE SENSOR BASED ON MAGNESIUM OXIDE-CHITOSAN NANOBIOCOMPOSITE FILM

P. D. KALE, A. B. BODADE, G. N. CHAUDHARI*

Nanotechnology Research Laboratory, Department of Chemistry, Shri Shivaji Science College, Amravati-444602(M.S), India

Received 02 Dec. 2016; Accepted 06 Jan. 2017

ABSTRACT

Nanoparticles play a major role in development of new hybrid composites for various engineering applications. A simple and novel amperometric biosensor for hydrogen peroxide detection is proposed. It is based on the immobilization of Horseradish peroxidase (HRP) in a chitosan (CH) matrix directly on a gold electrode surface (HRP/CH-NanoMgO/Au). Hydrogen peroxide was determined by direct electron transfer between the electrode surface and HRP. The MgO nanoparticles are prepared with sol-gel method. Synthesized nanoparticle was characterized by X-ray diffraction. XRD shows the average particle size was found to be ~ 16 nm for MgO. CH-NanoMgO/Au electrode and HRP/CH-NanoMgO/Au bioelectrode has been characterized by the scanning electron microscopy (SEM), Cyclic voltammetry (CV) demonstrated the fast electron transfer process between HRP and the electrode. The resulted H_2O_2 biosensor exhibited a rapid response upon the addition of H_2O_2, a low detection limit of 37.64 µM. The linear range of the biosensor is from 50-350 µM (R^2=0.97). A novel horseradish peroxidase (HRP) electrochemical biosensor based on a CH-NanoMgO/Au composite matrix was developed with easy preparation and low cost can provide a matrix for enzyme immobilization to construct biosensors with higher performance.

Keywords: Biosensor, MgO nanoparticles, Horseradish peroxidase (HRP), Chitosan (CH), Sol gel method.

INTRODUCTION:

Hydrogen peroxide (H_2O_2) is an essential component in food, biology, medicine, industry and environmental analysis. In addition, it is a byproduct of highly selective oxidases and an important contaminant in several industrial products and wastes [1]. It is also an excellent oxidizing and antibacterial property, H_2O_2 has been largely used in industries as an oxidizing agent [2], antibacterial agent [3] and bleaching agent [4]. Therefore, the accurate and convenient method for the determination of H_2O_2 is of great significance.

Amperometric biosensor is an attractive tool for the detection of H_2O_2. Other electrochemical methods such as cyclic voltammetry, linear sweep voltammetry and differential pulse voltammetry are also used for the development of H_2O_2 biosensor. HRP is one of the most extensively studied and commonly used enzymes for the construction of H_2O_2 biosensors. Horseradish peroxidase (HRP), a heme enzyme, is generally used as a enzyme to construct an efficient H_2O_2 biosensor for the determination of H_2O_2 or related compounds [5–8]. It can catalyze the oxidation of a wide variety of substrates by H_2O_2. Moreover, the reduced form of HRP can be chemically reoxidized by H_2O_2. In such peroxidase based biosensors, H_2O_2 is electroenzymatically reduced at low over potential due to the direct electron transfer between the electrode surface and HRP [9]. Accordingly, the fundamental principles for an electrochemical biosensor involve providing a suitable microenvironment for the enzyme to retaining its stability, bioactivity, accelerating the electron transfer between enzyme and electrode to realize the direct electrochemistry of enzyme. For achieving these goals, various materials have been utilized to modify the surface of electrode and immobilize HRP, including conducting polymers [10, 11], ionic liquid [12, 13] and biomolecule films [14, 15]. For example, Xiao et al. [16] used single-crystal CeO_2

*Corresponding author: G. N. CHAUDHARI | E-mail: gnchaudhari@gmail.com

nanocubes sol-gel for designing a H_2O_2 biosensor. Shan et al. [17] reported the immobilization of hemoglobin on nanoporous$CaCO_3$ films. Wang et al. reported the horseradish peroxidase amperometric biosensor based on a silica-hydroxyapatite hybrid film [7].

Magnesium oxide (MgO) it has received special attention because of its important applications in paints, catalysis toxic-water remediation, as additives in refractory, superconductor products and so on [18,19]. Despite versatile properties with various applications, there are few reports [20] on amperometric biosensors based on applications of MgO nanostructures. Due to the excellent film-forming ability, high permeability, and mechanical strength, biocompatibility, low cost and availability of chitosan has been found to be an interesting biopolymer for immobilization of biomolecules for biosensor applications. Chit is a kind of natural polysaccharide, which is derived from chitin, has good biocompatibility, biodegradability, low toxicity, good film forming character and anti-infective activity [21]. We report results of the studies carried out on immobilization and characterization of HRP on CH-NanoMgO composite film deposited onto gold plate using physical adsorption method.

EXPERIMENTAL

Materials

Chitosan (CHIT), Horseradish peroxidase (HRP), citric acid, ethyl alcohol, magenshium nitrate ($Mg(NO_3)_3.9H_2O$) were obtained from Sigma-Aldrich. Supporting electrolyte was (0.1 M) KCL containing 5 mM $[Fe(CN)_6]^{3-/4-}$. For phosphate buffer solution 50 mM of (pH 7.0), including disodium monohydroxy phosphate (Na_2HPO_4) and monosodium dihydroxy phosphate (NaH_2PO_4) were obtained from sigma. In all electrochemical tests double distilled deionized water was used. All other materials used in the laboratory were of analytical grade

Preparation of MgO nanoparticles

In Sol–gel synthesis stoichiometric ratio of AR grade magnesium nitrate ($Mg(NO_3)_3.9H_2O$) were dissolved in minimum amount of ethyl alcohol at room temperature and the sol was heated at 80^0 C on magnetic stirrer 3 hrs to form a wet gel. The gel was further heated in a pressure vessel at 130^0 C for 12 hrs. The combustion can be considered as a thermally induced redox reaction of the gel where in ethyl alcohol acts as a reducing agent. The nitrate ion acts as an oxidant. The obtained powder subjected to 3hrs heat treatment at 350^0 C in muffle furnace and then milled to a fine powder. The dried powder calcinated in range of 350^0-650^0 C in order to improve to the sensitivity and selectivity of material.

Preparation of biosensor

A chit solution was prepared by dissolving 0.5 mg/mL of chit flakes into 10 mL acetate buffer of 0.05M at pH 4.2 under continous stirring for 3 h at room temperature until complete dissolution. The prepared nanoparticles is dispersed in this solution. Finally, viscous solution of chit with uniformly dispersed MgO nanoparticles is obtained. CH-NanoMgO hybrid nanocomposite film have been fabricated by unifomaly 10 µL solution of CHIT- NanoMgO composite onto gold (Au) surface and allowing it to dry at room temperature for 12 h. These solution cast CH-NanoMgO hybrid nanocomposite film are washed repeatedly with deionized water to remove any unbound particles. Next, prepare the 10 µL of bioenzyme solution containing peroxidase (10 mg/ml) [prepared in phosphate buffer (5 mM)] is immobilized onto CH-NanoMgO electrode. The peroxidase immobilized CH-NanoMgO bioelectrode are kept undisturbed for about 12 h at 4°C. Finally, the dry bioelectrode is immersed in 50 mM PBS (pH 7.0) in order to wash out any unbound enzymes from the electrode surface (Fig. 1).

© 2017 All Rights Reserved.

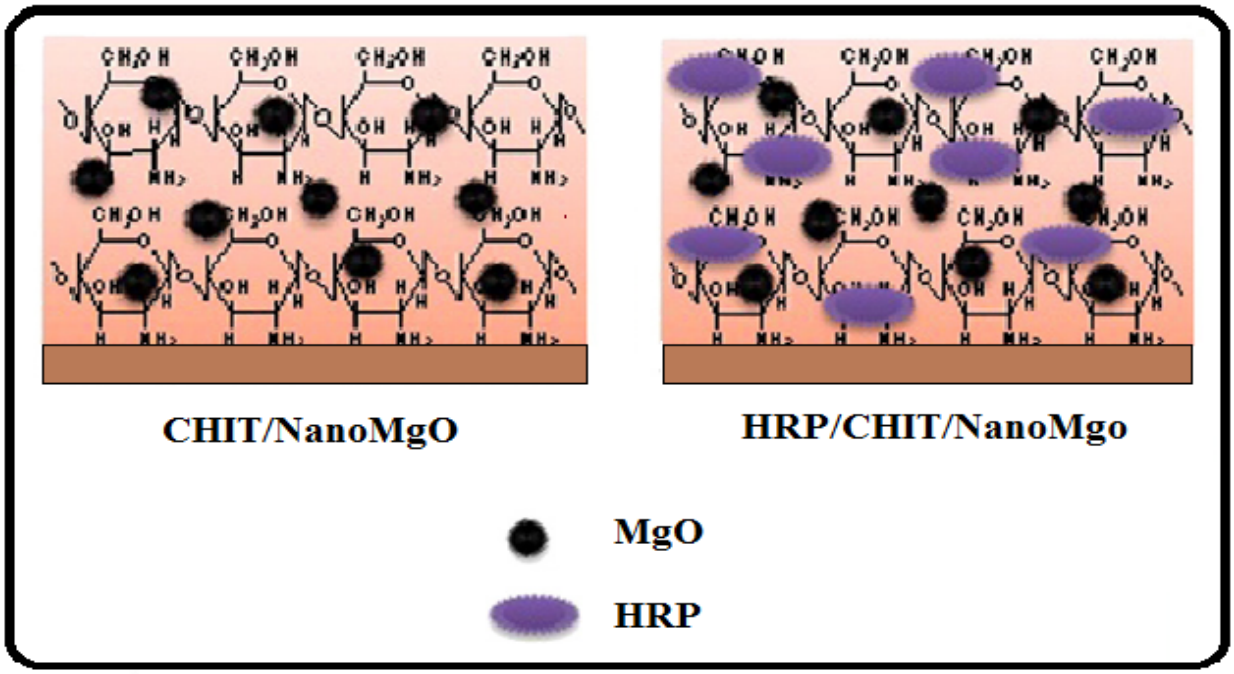

Figure 1: Illustrations of CH/NanoMgO electrode and HRP/CH-NanoMgO bioelectrode coated gold (Au) plate

Charcterzation

X-ray diffraction (XRD, Cu Ka radiation) study was performed to identify the crystal structure of MgO nanoparticles. Scanning electron microscopy (SEM-ZISS) studies were conducted to examine the surface morphology. Formation of MgO is also confirmed by the FT-IR spectroscopy. Electrochemical measurements were conducted on an using a three-electrode cell containing Au act as a working electrode, Ag/AgCl as reference electrode and platinum (Pt) wire serve as a counter electrode in KCL (0.1 M) containing 5 mM $[Fe(CN)_6]^{3-/4-}$ as the electrolyte. All amperometric measurements were carried out at room temperature.

RESULT AND DISCUSSION

XRD pattern of MgO Nanopaticles

The XRD pattern of MgO nanoparticles obtained from sol-gel method were as shown in (Fig. 2). The existence of strong and sharp diffraction peaks located at the 2θ value of 37.1^0, 43.1^0, 62.5^0 corresponding to (1 1 1), (2 0 0) and (2 2 0) planes respectively indicated the formation of MgO [22]. The result showed that the structure was in cubic structure and these results were matched with JCPDS data [JCPDS file: 45-0946] [23]. The crystalline size of MgO calculated using Debye Scherer's equestion,

$$D = \frac{K\lambda}{\beta cos\theta}$$

Where K is a constant equal to 0.89, β is the full width half maximum height of the diffraction peak at an angle θ and λ is wavelength. The average particle size of the MgO nanomaterials was found to be ~16 nm. Table 1 indicates the average particle size of the MgO samples.

Table 1: Particle size determination from XRD data

Obs. Max	Max Int (a.u.)	FWHM (θ)	Partical Size
37.1	113	0.55	15.91
43.1	1016	0.5	17.85
62.5	575	0.8	12.14

© 2017 All Rights Reserved.

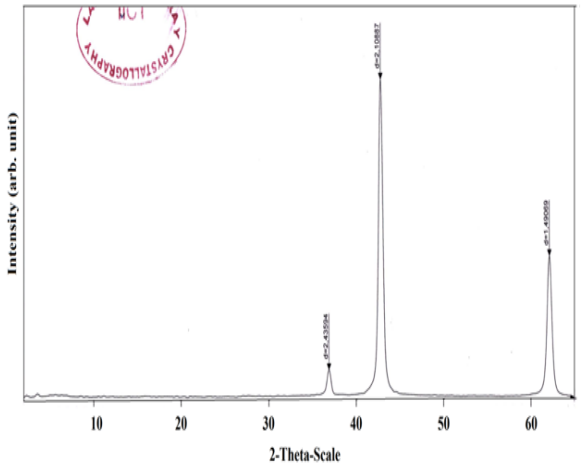

Figure 2: X-ray diffraction pattern of MgO particle

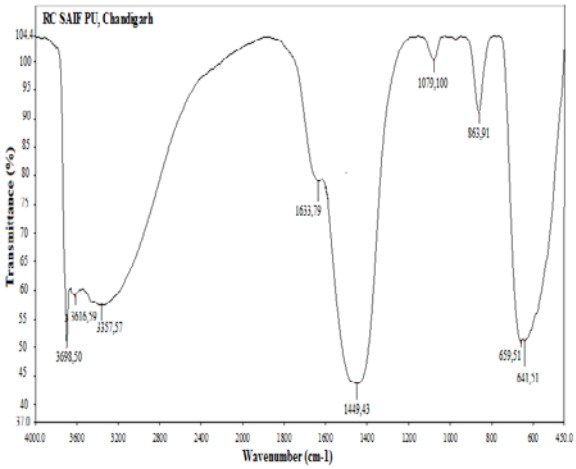

Figure 3: Fourier transformed infrared spectroscopy of MgO particles

Fourier transformed infrared spectroscopy (FT-IR)

FTIR spectra of MgO particles are shown in (fig. 3). In the wave number range 4000 to 400 cm^{-1}. The region between 3000- 4000 cm^{-1} shows the stretching mode of vibration in hydroxyl group (O-H). Peaks at 3698 cm^{-1}, 3616 cm^{-1} and 3357 cm^{-1} corresponding to the O-H stretching mode of hydroxyl groups. Peak at 1633 cm^{-1} was attributed to the bending vibration of water molecule. The major peaks at 641 cm^{-1}, 659 cm^{-1}, 863 cm^{-1} which confirmed the presence of mg-o vibrations [24, 25].

Surface morphology studies (SEM)

SEM study was employed to investigate the surface morphology of MgO nanoparticles, CH-NanoMgO/Au electrode and HRP/ CH-NanoMgO/Au bioelectrode are shown in fig. 4. The morphology of Mgo nanoparticles which indicate uniform in size and irregular fragments is shown in fig. 4a. The micrograph of a CH-NanoMgO/Au electrode appears to be a smooth surface. The adsorption of Horseradish peroxidase (HRP) enzyme onto the surface of sol-gel derived NanoMgO/Au is dependent on the morphology of the substrate. It can be seen that after immobilization HRP onto NanoMgO/Au electrode, shows a rough surface with spherical granules structure, indicating that HRP was entrapped in the NanoMgO/Au bioelectrode.

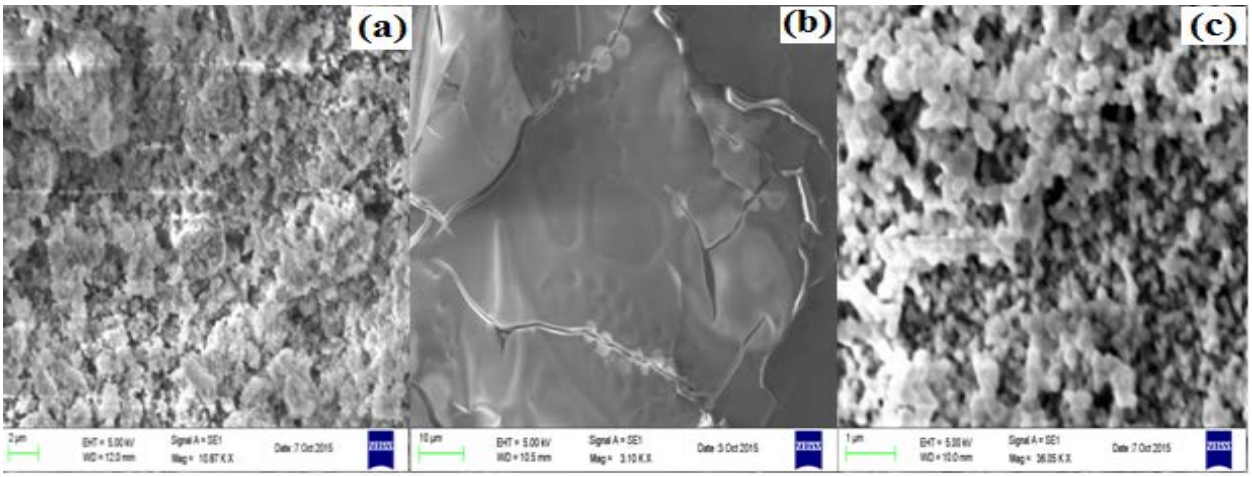

Figure 4: SEM of (a): MgO nanoparticles (b): CH-NanoMgO/Au electrode (c): HRP/CH-NanoMgO /Au bioelectrode

© 2017 All Rights Reserved.

Electrochemical Impedance Spectroscopy (EIS) of CH-NanoMgO/Au electrode and HRP/CH-NanoMgO /Au bioelectrode

Fig. 5 shows the real and imaginary parts of the impedance spectra represented as Nyquist plots (Zim vs. Zre) for CH-NanoMgO/Au and HRP/ CH-NanoMgO/Au bioelectrode in (0.1 M) KCL containing 5 mM $[Fe(CN)_6]^{3-/4-}$. The Nyquist plot of the EIS includes a semicircle part corresponds to electron-transfer limited process as its diameter is equal to the electron transfer resistance (RCT) that controls electron transfer kinetics of the redox probe at the electrode interface. The semicircle of the CH-NanoMgO/Au electrode decreased dramatically compared with HRP/CH-NanoMgO/Au bioelectrode, which indicates that the adsorption of HRP on nano-MgO made the semicircle increase again, indicating that HRP had been successfully immobilized.

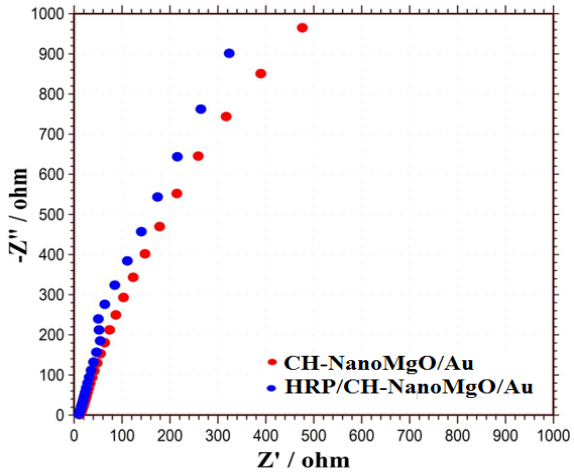

Figure 5: Nyquist plots of (a): CH-NanoNiFe$_2$O$_4$/Au electrode (b): HRP/CH-NanoMgO/Au bioelectrode in KCL (0.1 M) containing 5 mM$[Fe(CN)_6]^{3-/4-}$

Direct Electron Transfer from HRP to the Surface of HRP/ CH-NanoMgO/Au

The changes of electrode behavior after surface modification with enzymes (HRP) were studied by cyclic voltammetry (CV) in the presence of ferricyanide mediator. The electrode surface is modified by the biocatalytic material, the change in the electron transfer kinetics of $[Fe(CN)_6]^{3-/4-}$ gives indication of the enzyme attachment. The electrochemical studies of both CH-NanoMgO/Au electrode and HRP/CH-NanoMgO/Au bioelectrode have been studied using cyclic voltammetry in (0.1 M) KCL containing 5 mM $[Fe(CN)_6]^{3-/4-}$.

In fig. 6 observed that the CH-NanoMgO/Au electrode shows oxidation reduction peaks after the immobilization of HRP on the CH-NanoMgO/Au bioelectrode redox peak are increases. Cathodic and Anodic peaks were located at 0.220 V and 0.100 V, respectively which indicates stable immobilization of HRP and MgO nanoparticles on the surface of Au (gold) electrode. Here the role of MgO nanoparticles is to facilate and accelerate electron transfer rate between heme group of enzyme and Au.

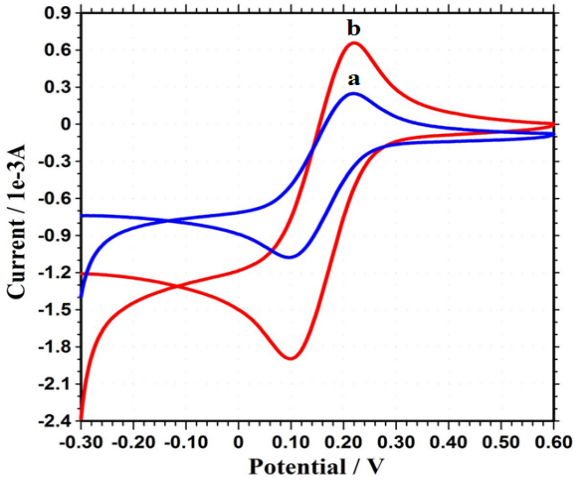

Figure 6: Cyclic voltammogrammes of (a): CH-NanoMgO /Au (b): HRP/CH-NanoMgO /Au HRP/CH-NanoMgO /Au bioelectrode at 0.01 V/s

Fig. 7 (a) demonstrates typical CV of HRP/ CH-NanoMgO/Au bioelectrode with scan rate varying from 0.01 to 0.07 V/s. With increase in the scan rate, there is increase in both the cathodic and anodic peak current accompanied with small shift and increased peak-to-peak separation indicating a surface controlled electrode process. This reveals that the electron transfer between enzyme and electrode could be easily performed and it was a surface confined electrochemical process. To analyze this part of electrochemical studies in more detail, the data obtained in fig. 7b (based on scan rate, *v*) and 7c (based on square root of scan rate, $v^{1/2}$ $s^{-1/2}$). It is seen that redox peaks show a linear increase and the obtained correlation coefficient for cathodic and anodic peaks are equal to 0.992 (ipc = 15.94 - 0.094) and 0.992 (ipa = -

© 2017 All Rights Reserved.

14.82 V-0.945), respectively. These values confirm proper and stable immobilization of HRP on the surface of CH-NanoMgO/Au and also effective role of MgO nanoparticles as facilitators of direct electron transfer process. Results of this part of studies can be used to determine the amount of enzyme in potassium chloride. Besides, the redox peak currents are proportional to the square root of scan rate ($v^{1/2}$ $s^{-1/2}$), indicating a diffusion electron-transfer process it can be seen (Fig. 7c).

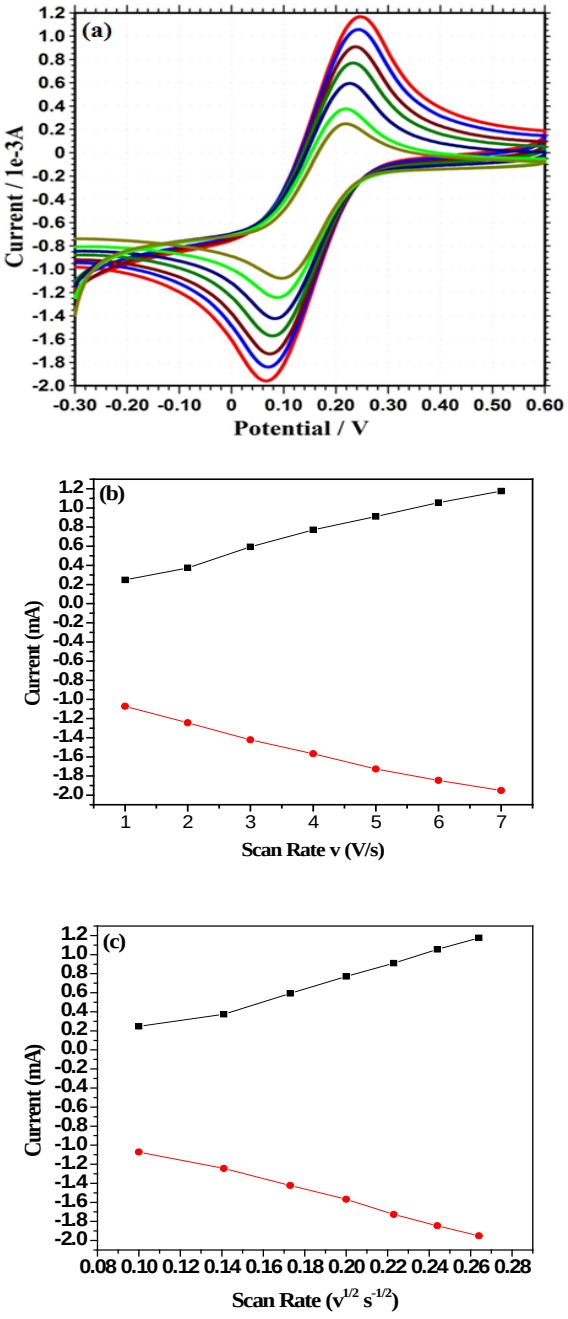

Figure 7: (a) CV of HRP/CH-NanoMgO /Au Relationship of cathodic and anodic peak currents (b) with scan rate (v) (c) square root of scan rate ($v^{1/2}$ $s^{-1/2}$) at different scan rate (0.01-0.06 V/s)

The values of heterogeneous electron transfer rate constant *(k_s)* of HRP immobilized CH-NanoMgO /Au bioelectrode have been calculated using the Laviron model [26].

$$k_s = \frac{mnFv}{RT}$$

Where, m is peak-to-peak separation, *F* is Faraday constant, v is scan rate (mV/s), n is the number of transferred electrons and R is gas constant. The value of k_s obtained as 0.0467 s^{-1} (T = 298 K, n = 1, m = 0.120 V and v = 10 mV/s) indicating fast electron transfer between immobilized HRP and electrode due to the presence of MgO nanoparticles in the CH-NanoMgO nanobiocomposite.

The surface concentration of the HRP/CH-NanoMgO /Au film can be estimated from the plot of current (I_P) vs scan rate (v/s) using Brown-Anson model that is based on the following equation Fig. (7b). The value estimated for the number of electrons, n =1, was therefore used to calculate the surface concentration of electroactive HRP the CH-NanoMgO film. For thin layer electrochemical behaviour like that exhibited by HRP, the surface concentration (*I**) of its electroactive species in the mediator or promoter used can be deduced by integration of the peaks of the cyclic voltammograms of the biosensor Fig. (7b).

$$I_P = \frac{n^2F^2I^*Av}{4RT}$$

Where A is the surface area of the electrode (1 cm^2), *n* is the number of electrons transferred which is 1, *F* is the Faraday constant (96.5 KJ mol^{-1}), I* is the surface concentration (mol cm^2) obtained for the HRP/CH-NanoMgO /Au bioelectrode, From the slope of the Ip-v curve for a surface process, *R* is the gas constant (8.314 J^{-1} mol K), and *T* is the absolute temperature (298 K). The value of the surface concentration of the HRP/CH-NanoMgO /Au bioelectrode has been found to be 8.77 × 10^{-6} mol cm^{-2}. This implies that multiple layers of HRP were immobilized on the CH film. Also the ability of the CH-NanoMgO to maintain electro activity and conductivity in neutral media play as effective electron transfer mediators for the construction of biosensors.

The Randel-Sevcik equation was used to determine the diffusion coefficient of the electrons (D) of HRP/CH-NanoMgO /Au bioelectrode can be evaluated from the slope of the straight line

© 2017 All Rights Reserved.

obtained from the current (I_P) vs. square root of scan rate, ($v^{1/2}$) plot in (Fig. 7c) and was equivalent to $4.38 \times 10^{-5} cm^2 s^{-1}$.

$$i_p = (2.69 \times 10^5) n^{3/2} A D^{1/2} C v^{1/2}$$

Where D value depends on the density and homogeneity of the film as well as other conditions for growing the polymer. This provides an indication of the diffusion controlled nature of the cathodic peak current arising from the electron propagation through the polymer chain.

Electrochemical Response Studies

In the response study detecting H_2O_2 in ranges as small as 50-350 µM concentrations in biological, medical and industrial activities is quite obvious. In detection of H_2O_2 different methods are used such as spectrometry, chemiluminescence and electrochemistry are employed [27]; yet a more suitable and efficient choice is electrochemical processes, as they offer greater sensitivity and selectivity compared to other methods. In present research various concentrations of H_2O_2 were added in the presence of HRP/CH-NanoMgO/Au bioelectrode (0.1 M) KCL containing 5 mM $[Fe(CN)_6]^{3-/4-}$. In fig. (8a) results revealed that as concentration of H_2O_2 is increased, the height of cathodic peak also increases while that of anodic peak is decreased. In this section of the research it was found that sensitivity and reactivity to H_2O_2 happens only when all the three factors (i.e., Au plate, MgO NPs and HRP enzyme) are used together. The H_2O_2 reduction was triggered by the electrocatalysis from HRP– Fe(II) of HRP, which could reduce H_2O_2 while being oxidized to HRP–Fe(III) and then quickly reduced back to HRP–Fe(II) through its direct electron transfer ability with the electrode [28]. The electrocatalytic process could be expressed as follows:

HRP-Fe (II) + H_2O_2 ⟶ HRP-Fe (III) + H_2O

HRP-Fe (III) + e^- ⟶ HRP-Fe (II)

Such a process provides firm evidence for the catalytic effect of HRP and its proper immobilization on the surface of CHIT-NanoMgO/Au, where the process of electron transfer has been facilitated by MgO NPs.

Fig. 8(b) shows calibration plot between current over the concentration range 50-350 µM. Sensitivity of prepared bioelectrode is found to be 0.001 mA $\mu M^{-1} cm^{-2}$ which is calculate from slope of plot current verses concentration, a correlation coefficient of 0.995 and the detection limit of 37.64 µM. An extremely attractive feature of the enzyme electrode, is its fast response time (i.e. 2s). The relationship between the catalytic current and the concentration of H_2O_2 shows a Michaelis – Menten kinetic mechanism. The apparent Michaelis–Menten constant (K_{mapp}) could be calculated from the Lineweaver –Burk equation [29]:

$$1/I_{ss} = 1/I_{max} + K_{mapp}/I_{max}C$$

where I_{max} and C represent the steady current, maximum current and H_2O_2 concentration, respectively. According to the intercept and slope of above regression equation, K_{mapp} can be estimated to be 0.14 mM. The small apparent Michaelis –Menten constant shows a high affinity to H_2O_2 and good bioactivity of HRP/nano-MgO/chit toward H_2O_2 reduction.

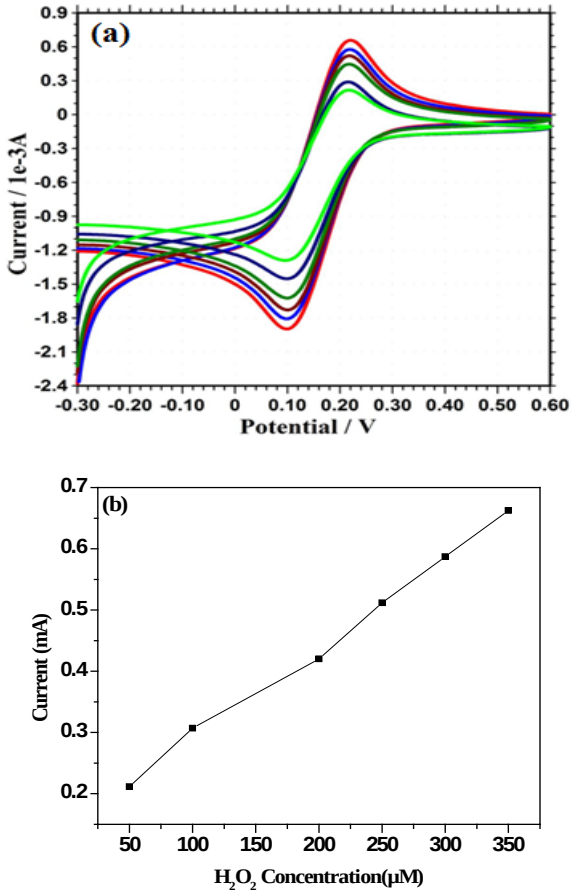

Fig. 8: (a) Electrochemical response of HRP/CH-NanoMgO /Au bioelectrode as a function of H_2O_2 concentration (b) Calibration curve between current response and different concentrations of H_2O_2 in KCL (0.1 M) containing 5 mM $[Fe(CN)_6]^{3-/4-}$.

© 2017 All Rights Reserved.

CONCULSION

The MgO were successfully prepared by a sol-gel method and utilized to immobilize HRP for constructing a novel H_2O_2 biosensor. Due to their unique properties, the MgO suggested immobilization matrix provided a mild immobilization process for HRP and enhanced the electron transfer between the enzyme active sites and the electrode. The direct electrochemistry and high electrocatalytic activity to the reduction of H_2O_2 of HRP was demonstrated. The resulted biosensor based on the composites exhibited high sensitivity, low detection limit, wide linear range, and long term stability. The resulting biosensor exhibited showed good performances in the determination of H_2O_2 with linear range of 50-350 µM (R^2=0.97) and low detection limit of 37.64 µM.

ACKNOWLEDGEMENT

The authors are also indebted to Principal, Dr. V. G. Thakare, Shri Shivaji Science College Amravati, India for his kind cooperation during this research work. This work was financially supported by Major Research Project (No.43-224/2014(SR)) sanctioned by University Grants commission (UGC), New Delhi, India.

REFERENCES

1. Camacho C, Matias JC, Chico B, Cao R, Go´mez L. Amperometric biosensor for hydrogen peroxide, using supramolecularly immobilized horseradish peroxidase on the β-cyclodextrin-coated gold electrode, Electroanalysis., 2007;19: 2538-2542.
2. Yeh CK, Wu H, Chen T. Chemical oxidation of chlorinated non-aqueous phase liquid by hydrogen peroxide in natural sand systems, Journal of Hazard. Mater., 2003; 96 (1): 29-51.
3. Weston RJ. The contribution of catalase and other natural products to the antibacterial activity of honey: a review Food Chem., 2000; 71 (2): 235-239.
4. Moore DB, Argyropoulos DS. Determination of Peroxygen Species Present in Pulp Fiber Matrixes, Anal. Chem., 1999;71 (1) :109-114.
5. Xu J, Zhu J, Wu Q, Hu Z, Chen H. An Amperometric Biosensor Based on the Coimmobilization of Horseradish Peroxidase and Methylene Blue on a Carbon Nanotubes Modified Electrode, Electroanalysis., 2003; 15 (3) : 219-224.
6. Maduraiveeran G, Ramaraj R. A facile electrochemical sensor designed from gold nanoparticles embedded in three-dimensional sol–gel network for concurrent detection of toxic chemicals, Electrochem. Commun., 2007; 9 (8): 2051-2055.
7. Wang B, Zhang J, Pan Z, Tao X, Wang H. A novel hydrogen peroxide sensor based on the direct electron transfer of horseradish peroxidase immobilized on silica–hydroxyapatite hybrid film, Biosens. Bioelectron., 2009; 24 (5): 1141-1145.
8. Li L, Huang J, Wang T, Zhang H, Liu Y, Li J. An excellent enzyme biosensor based on Sb-doped SnO_2 nanowires, Biosens. Bioelectron., 2010; 25 (11): 2436-2441.
9. Dzyadevych SV, Arkhypova VN, Soldatkin AP, Elskaya AV, Martelet C, Jaffrezic-Renault N. Amperometric enzyme biosensors: Past, present and future. ITBM-RBM,: 2008;29 :171-180.
10. Kong YT, Boopathi M, Shim YB. Direct electrochemistry of horseradish peroxidase bonded on a conducting polymer modified glassy carbon electrode. Biosens. Bioelectron., 2003; 19 (3): 227-232.
11. Xua Q, Zhu JJ, Hu XY. Ordered mesoporous polyaniline film as a new matrix for enzyme immobilization and biosensor construction, Anal. Chim. Acta ; 2007; 597 (1) : 151-156.
12. Xi F, Liu L, Wu Q, Lin X. One-step construction of biosensor based on chitosan–ionic liquid–horseradish peroxidase biocomposite formed by electrodeposition. Biosens. Bioelectron, 2008; 24 (1) : 29-34.
13. Yan R, Zhao FQ, Li JW, Xiao F, Fan SS, Zeng BZ. Direct electrochemistry of horseradish peroxidase in gelatin-hydrophobic ionic liquid gel films. Electrochim. Acta; 2007; 52 (26): 7425-7431.
14. Song YH, Wang L, Ren CB, Zhu GY, Li Z. A novel hydrogen peroxide sensor based on horseradish peroxidase immobilized in DNA films on a gold electrode, Sens. Actuators B;, 2006; 114 (2): 1001-1006.
15. Tang JL, Wang BQ, Wu ZY, Han XJ, Dong SJ, Wang EK. Lipid membrane immobilized horseradish peroxidase biosensor for amperometric determination of hydrogen peroxide Biosens, Bioelectron., 2003; 18 (7), 867-872.

© 2017 All Rights Reserved.

16. Xiao XL, Luan QF, Yao X, Zhou KB. Single-crystal CeO_2 nanocubes used for the direct electron transfer and electrocatalysis of horseradish peroxidase, Biosens. Bioelectron., 2009; 24 (8): 2447-2451.

17. Shan D, Wang SX, Xue HG, Cosnier S. Direct electrochemistry and electrocatalysis of hemoglobin entrapped in composite matrix based on chitosan and $CaCO_3$ nanoparticles. Electrochem. Commun., 2007; 9 (4):529-534.

18. Yin Y, Zhang G, Xia Y. Synthesis and characterization of MgO nanowires through a vapor-phase precursor method, Adv. Funct. Mater., 2002; 12 (4); 293-298.

19. Yang Q, Sha J, Wang L, Wang J, Yang D. MgO nanostructures synthesized by thermal evaporation, Mater. Sci. Eng: C., 2006; 26 (5-7):1097-1101.

20. Umar A, Rahman MM, Hahn YB. MgO polyhedral nanocages and nanocrystals based glucose biosensor, Electrochem. Commun., 2009; 11 (7): 1353-1357.

21. Renbutsu E, Hirose M, Omura Y, Nakatsubo F, Okamura Y, Okamoto Y, Saimoto HY, Shigemasa S, Minami. Preparation and Biocompatibility of Novel UV-Curable Chitosan Derivatives, Biomacromolecules., 2005; 6 (5):2385-2388.

22. Ganguly A, Trinh P, Ramanujachary KV, Ahmad T, Mugweru A, Ganguli AK. Reverse mi-cellar based synthesis of ultrafine MgO nanoparticles (8–10 nm): Characterization and catalytic properties, J. Colloid. Interf. Sci., 2011; 353, 137–142.

23. Athar T, Hakeem A, Ahmed W. Synthesis of MgO Nanopowder via Non Aqueous Sol–Gel Method, Adv. Sci. Lett.; 2012; 5: 1-3.

24. Mehran R, Majid K, Behzad N. Synthesis of high surface area nanocrystalline MgO by pluronic P123 triblock copolymer surfactant, Powder Technol., 2011; 205: 112-116.

25. Guolin Song, Sude Ma, Guoyi Tang, Xiaowei Wang. Ultra-sonic-assisted synthesis of hydrophobic magnesium hydroxide nanoparticles., Colloids Surf. A., 2010; 364: 99-104.

26. Laviron E. General Expression of the linear potential sweep voltammogram in the of diffusionless electrochemical systems. J Electroanal Chem., 1979; 101:19-28.

27. Hadaegh A, Sayad A, Dastjerdi HA, Fazilati M, Zarchi SR. Direct Electron Transfer of Cytochrome c on ZrO2 Nanoparticles Modified Glassy Carbon Electrode, International Journal of Electrochemical Science., 2012; 7: 7033-7044.

28. Xiang C, Zou Y, Sun L, Xu F. Direct electrochemistry and enhanced electrocatalysis of horseradish peroxidase based on flowerlike ZnO–gold nanoparticle–Nafion nanocomposite. Sens. Actuators B., 2009; 136(1):158.

29. Kamin RA, Willson GS. Rotating ring-disk enzyme electrode for biocatalysis kinetic studies and characterization of the immobilized enzyme layer, Anal. Chem., 1980;52 (8): 1198-1205.

© 2017 All Rights Reserved.